Impaired neural response to speech edges in dyslexia

Mikel Lizarazu[1,2], Marie Lallier[1], Mathieu Bourguignon[3], Manuel Carreiras[1,4,5] & Nicola Molinaro[1,4]

[1]*BCBL, Basque center on Cognition, Brain and Language, Donostia/San Sebastian, Spain.*

[2]*LSCP, Département d'études cognitives, ENS, EHESS, CNRS, PSL Research University, 75005 Paris, France.*

[3]*Laboratoire de Cartographie Fonctionnelle du Cerveau, Hopital Erasme, Universite Libre de Bruxelles, Brussels, Belgium.*

[4]*Ikerbasque, Basque Foundation for Science, Bilbao, Spain.*

[5]*University of the Basque Country (UPV/EHU), Bilbao, Spain.*

SHORT TITLE:
Speech processing in dyslexia

KEYWORDS:
Dyslexia, phonological deficit, speech, neural oscillations, Magnetoencephalography

CORRESPONDING AUTHOR:
Mikel Lizarazu
69 Mikeletegi Pasealekua,
20009 San Sebastian, Spain
email: mikel.lizarazu@ens.fr phone: 943 30 93 00

Abstract

Speech comprehension has been proposed to critically rely on oscillatory cortical tracking, that is, phase alignment of neural oscillations to the slow temporal modulations (envelope) of speech. Speech-brain entrainment is readjusted over time as transient events (edges) in speech lead to speech-brain phase realignment. Auditory behavioral research suggests that phonological deficits in dyslexia are linked to difficulty in discriminating speech edges. Importantly, research to date has not specifically examined neural responses to speech edges in dyslexia. In the present study, we used MEG to record brain activity from normal and dyslexic readers while they listened to speech. We computed phase locking values (PLVs) to evaluate phase entrainment between neural oscillations and the speech envelope time-locked to edge onsets. In both groups, we observed that edge onsets induced phase resets in the auditory oscillations tracking speech, thereby enhancing their entrainment to speech. Importantly, dyslexic readers showed weaker PLVs compared to normal readers in left auditory regions from ~0.15 s to ~0.65 s after edge onset. Our results indicate that the neural mechanism that adapts cortical entrainment to the speech envelope is impaired in dyslexia. These findings here are consistent with the temporal sampling theory of developmental dyslexia.

Introduction

The speech signal includes slow temporal fluctuations in the 1 – 10 Hz band that are closely related to phrase and syllable features in the acoustic signal. Tracking such temporal structures, both at phrasal and syllabic rates, is crucial for speech segmentation (Greenberg et al., 2003; Poeppel, 2003; Poeppel, Idsardi, and van Wassenhove, 2008). The phase of low-frequency delta (1 – 3 Hz) and theta (4 – 7 Hz) oscillations in auditory cortex synchronizes to the phrasal and syllabic patterns of speech, respectively (Molinaro and Lizarazu, 2018; Lizarazu, Lallier and Molinaro, 2019; Bourguignon et al., 2013). The theta band effect has been interpreted as a basic auditory mechanism exogenously "entrained" by the syllabic structure of the speech envelope, while the delta effect also involves endogenous attentional mechanisms (Molinaro and Lizarazu, 2018; Meyer, Sun and Martin, 2019; Obleser and Kayser, 2019; Donhauser and Baillet, 2019). Optimal neural synchronization to different speech rhythms depends on rapid neural responses to large-amplitude transients ("edges"), visible in the speech envelope (*Top-Left*, Figure 1). Speech edges phase-reset low-frequency (delta and theta) oscillations in auditory regions, thus improving alignment to the speech envelope (Gross et al., 2013a). In other words, speech edges function as temporal landmarks for cortical speech tracking mechanisms that periodically re-adjust speech-brain synchronization to ensure high temporal precision. Gross and colleagues (2013a) reported that increased speech-brain coupling in the theta band peaked around 0.1 seconds after speech edges, similar to evoked electrophysiological responses to auditory stimuli. This synchronization decreased over time, but continued to index robust speech-brain coupling, tracking the speech envelope. This neural mechanism optimizes speech segmentation and sampling thus improving phonological information processing (Doelling et al., 2014).

Previous research has suggested that there are three subtypes of dyslexia: phonological, surface and mixed (Castles and Coltheart, 1993; Manis et al., 1996). Phonological dyslexia is characterized by a difficulty in reading pseudowords; surface dyslexia by a difficulty in reading irregular words. Individuals with mixed dyslexia exhibit symptoms of both surface and

phonological dyslexia. However, more recently other studies support the hypothesis that a phonological deficit lies at the core of developmental dyslexia, challenging the idea that there is a clear dissociation between the surface and phonological profiles (Sprenger-Charolles and Serniclaes, 2003; Ramus et al., 2003). This debate remains a major theoretical and clinical issue, along with the prevalence of these profiles and the variation in that prevalence depending on the orthographic transparency of a language, the employed experimental design and the measures obtain from the phonological and reading tasks or how the control participants are matched (Sprenger-Charolles, 2011; Sohrabi and Sohrabi, 2017).

Phonological difficulties in dyslexia have been linked to poor synchronization between the speech envelope and oscillatory cortical activity. The "temporal sampling framework" (Goswami, 2011) proposes that the auditory perceptual deficits observed in dyslexia are linked to atypical neural entrainment of low-frequency oscillations to the slow amplitude modulations in speech. Recent neuroimaging studies (see Jiménez-Bravo, Marrero and Benítez-Burraco, 2017 for a recent review) have found that dyslexic readers showed weaker speech-brain coupling than normal readers, mainly in the delta band and right auditory cortex (Cutini et al., 2015; Molinaro et al., 2016; Power et al., 2013, 2016). In the theta band, evidence for atypical neural synchronization in the auditory cortex of dyslexic readers is not conclusive (Hämäläinen et al. 2012; Lizarazu et al., 2015; De Vos et al., 2017a, b). Using non-speech sounds (amplitude modulated (AM) white noise), De Vos and colleagues (2017a) found that dyslexic readers showed weaker neural entrainment than normal readers at 4 Hz AMs. Conversely, Lizarazu and colleagues (2015) reported stronger auditory entrainment in dyslexic readers at 4 Hz AMs. In terms of strictly syllabic speech tracking, no differential effects between dyslexic and control readers have been observed in the theta band.

Atypical speech-brain coupling in dyslexia could potentially be linked to the reported deficit in processing speech edges (more specifically, 'rise-times') in these populations (e.g. Goswami et al., 2002, 2011; Richardson et al., 2004; Thomson and Goswami, 2008; Thomson, Goswami and

Baldeweg, 2009; Leong and Goswami, 2014; Van Hirtum et al., 2019a, b). The perceptual consequences of reduced sensitivity to the temporal profile of speech edges includes difficulty perceiving speech rhythms, and poorer segmentation of the speech stream at the prosodic and syllabic levels (Greenberg et al., 2003). In a recent behavioral study, Van Hirtum and colleagues (2019a) used a speech envelope enhancement strategy to reduce speech perception deficits in adults with dyslexia. This envelope enhancement strategy emphasizes onset edges cues and specifically reinforces the temporal structure of the speech envelope. They found that dyslexic readers not only benefited from envelope enhancement but benefited from it more than normal readers. In fact, envelope enhancement completely normalized speech reception thresholds for dyslexic readers under adverse listening conditions. It is interesting to note that the benefits of these simple sensory enhancement strategist emerge in adults, whose auditory system is already well-developed. The same group (Van Hirtum et al., 2019b) also analyzed neural synchronization in normal and dyslexic readers using auditory steady-state EEG responses at theta, alpha, beta, and low-gamma range oscillations (i.e., 4, 10, 20 and 40 Hz) to stimuli with different rising edges. They found reduced neural synchronization in the alpha, beta, and low-gamma frequency ranges in dyslexia. Moreover, atypical neural synchronization was modulated by rise time for alpha and beta oscillations, showing that deficits found at 10 and 20 Hz were only evident when the envelope's rise time was significantly shortened. Importantly, Van Hirtum and colleagues (2019b) analyzed neural responses to non-linguistic audio stimuli (amplitude modulated white-noise) and not to natural speech. It is thus possible that the effects for alpha and beta oscillations could reflect attentional components of these stimuli, and that these effects are not present for real speech.

Before extracting the meaning of an utterance, speech-entrained brain oscillations at different frequency bands are hierarchically coupled to mediate the encoding of the phonological structure of continuous speech (Leong and Goswami, 2015). Specifically, the phase of low-frequency (delta and theta) oscillations modulates the amplitude of high-frequency (gamma)

oscillations in auditory regions (Poeppel, 2003; Gross et al., 2013a; Lizarazu, Lallier and Molinaro, 2019). Furthermore, speech edges increase phase amplitude cross-frequency coupling between multiple frequency channels, enhancing the temporal precision of these multi-scale nested dependencies (Gross et al., 2013a). Atypical delta and theta synchronization to speech edges could in fact affect higher frequency oscillations just because low-frequency oscillations constitute the first level within the hierarchical coupling.

In the present study, we evaluated whether neural mechanisms involved in phase realignment to speech edges are affected in developmental dyslexia. We measured the magnetoencephalographic (MEG) brain response elicited by speech edges in normal and dyslexic readers. Specifically, we evaluated phase-locking between neural oscillations and the speech envelope time-locked to edge onsets. Based on previous studies (Gross et al., 2013a), we expected that edges in the speech would phase reset auditory cortex oscillations and enhance their entrainment to speech. Furthermore, in line with Goswami´s theory, we hypothesized that dyslexic readers would present reduced sensitivity to speech edges and, consequently, weaker coupling between low-frequency auditory oscillations and speech.

Material and Methods

Participants

Thirty-six participants took part in the present study, including 18 skilled readers (10 females) and 18 dyslexic readers (9 females). Participants' ages ranged from 16.8 to 44.9 years (skilled readers) and from 17.2 to 44.9 years (dyslexic readers). Subjects in both groups were matched in age (p = 0.75). Inclusion criteria required participants (a) to be a native Spanish speaker; (b) to report no neurological/psychiatric disorders; (c) not to be under the influence of psychoactive drugs, (d) to have normal or corrected-to-normal vision and no hearing impairment and (e) to have a non-verbal IQ greater than or equal to 85. All participants were Spanish monolinguals, reported no hearing impairments, and were right-handed. Auditory tests were carried out by these pedagogues and normal hearing was required for the neuroimaging experiments. The dyslexic readers were selected by a group of trained therapists from the University of Oviedo. All of the dyslexic participants taking part in this study showed reading and/or writing difficulties and had received a formal diagnosis of dyslexia from a qualified practitioner. None of the normal readers reported reading or spelling difficulties or had received a formal diagnosis of dyslexia. Inclusion and exclusion criteria for the participants selection were established prior to data analysis.

The present experiment was undertaken with the understanding and written consent of each participant. The Basque Center on Cognition Brain and Language (BCBL) ethical committee approved the experiment (following the principles of the Declaration of Helsinki).

Behavioral data

Intelligence quotient (IQ)

The Wechsler Adult Intelligence Scale' (WAIS) test (Wechsler, 2008) was used to estimate the intelligence quotient (IQ) levels in all participants.

Reading task

Reading performance was evaluated with the word and pseudoword reading list of the PROLEC-R battery (Cuetos et al., 2007). For each list, accuracy and total time to read the list were measured. Then, z-scores based on the performance of 46 skilled monolingual Spanish adults matched for age (M=32.5; SD=11.6) were computed for the control and dyslexic groups of the present study (all *p*s > 0.2).

Phonological processing tasks

Pseudoword repetition (phonological short term memory)

Participants listened to 24 pseudowords successively presented over headphones and were told to repeat them as accurately as possible. There were 3 sets of pseudowords, respectively composed of 2, 3, and 4 syllables. Pseudoword structure followed Spanish phonotactic rules and did not include repetition of any phonemes. The number of correctly repeated pseudowords was recorded and converted into percentage of accuracy. Phonemic errors were then analyzed and coded as one of four categories: (e.g., phonemic permutation (/mus***b***o***l***ife/ → /mus***l***o***b***ife/), phonemic addition (/ta***Ø***forbegun/→/ta***s***forbegun/), phonemic substitution (/***t***alsomen/→ /***k***alsomen/), and phonemic omission (/taforbegu***n***/ → /taforbegu***Ø***/).

Phonemic deletion (phonemic awareness)

Participants listened to pseudowords through headphones. They were told to remove the first sound of the pseudoword and produce what remained. Twenty-four pseudowords were presented. All the pseudowords were composed of 2 syllables that respected Spanish phonotactic rules. Half of the pseudowords started with a simple consonant-vowel syllable (e.g., /pa/) and the remaining half started with a consonantal cluster (e.g., /tr/). The number of correct responses was recorded and converted into percentage of accuracy. Phonemic errors were then analyzed and coded as one of two categories: phoneme deletions errors (e.g., /***pl***adi/ → /adi/) and phonemic errors occurring outside of the deletion site (e.g., /***pl***adi/ → /lati/).

Statistical analysis

For each measure collected from the behavioral tasks, differences between groups were determined using a t-test (2-tailed, unequal variance).

Neurofunctional data

Participant´s brain activity was recorded using Magnetoencephalography (MEG). MEG is a completely non-invasive neuroimaging technique. MEG measures magnetic fields produced by the electrical activity of neurons. MEG offers a way to localize brain activity with high spatial and temporal resolution (Hämäläinen et al., 1993; Gross et al., 2013b).

Stimuli and Procedure

The stimuli consisted of 35 meaningful semantically neutral sentences ranging in duration from 7.4 to 12.7 s (M = 9.9; SD = 1.1). Sentences were uttered by a Spanish native female speaker and digitized at 44.1 kHz using a digital recorder (Marantz PMD670). Audio files (*.wav) were segmented using Praat (Boersma and Weenink, 2018). Sentences were normalized by peak amplitude to ensure equal maximum volume for all stimuli. Peak normalization was based on the highest signal level present in each sentence.

During MEG recording, sentences were presented auditorily to the participants at 75 decibel (dB) sound pressure level (SPL). Each trial began with a 1-s auditory tone (at 500 Hz) followed by a 2-s silence before the sentence presentation. A comprehension question about the content of the last stimulus was presented auditorily 2 s after the end of each sentence. During sentence presentation, participants were asked to fixate a white-color sticker on the switched-off screen. Participants answered the question by pressing the appropriate button (Yes/No). After response, the next trial was presented. Response hands for Yes/No responses were counterbalanced across participants and the presentation order of the sentences was randomized. The percentage of correct responses to comprehension questions was very high in both normal (M = 98%, SD = 4%) and dyslexic readers (M = 97%, SD = 3%). Participants were asked to avoid head movements and to try to blink only during time periods between sentences.

Stimuli were delivered using Presentation software (Version 16.5 Neurobehavioral Systems, Inc., Berkeley, CA, USA; http://www.neurobs.com/).

Data acquisition and preprocessing

MEG data were acquired in a magnetically shielded room using the whole-scalp MEG system (Elekta-Neuromag, Helsinki, Finland) installed at the BCBL: http://www.bcbl.eu/bcbl-facilitiesresources/meg/). The system is equipped with 102 sensor triplets (each comprising a magnetometer and two orthogonal planar gradiometers) uniformly distributed around the head of the participant. Head position inside the helmet was continuously monitored using four Head Position Indicator (HPI) coils. The location of each coil relative to the anatomical fiducials (nasion, left and right preauricular points) was defined with a 3D digitizer (Fastrak Polhemus, Colchester, VA, USA). This procedure is critical for head movement compensation during the data recording session. Digitalization of the fiducials plus ~100 additional points evenly distributed over the scalp of the participant were used during subsequent data analysis to spatially align the MEG sensor coordinates with T1 magnetic resonance brain images acquired on a 3T MRI scan (Siemens Medical System, Erlangen, Germany). MEG recordings were acquired continuously with a bandpass filter at 0.01-330 Hz and a sampling rate of 1000 Hz. Eye movements were monitored with two pairs of electrodes in a bipolar montage placed on the external chanti of each eye (horizontal electrooculography (EOG)) and above and below right eye (vertical EOG).

Figure 1 illustrates the processing of the MEG and speech signals. To remove external magnetic noise from the MEG recordings, data were preprocessed off-line using the Signal-Space-Separation (SSS) method (Taulu and Kajola, 2005) implemented in Maxfilter 2.1 (Elekta-Neuromag). MEG data were also corrected for head movements, and bad channel time courses were reconstructed using interpolation algorithms implemented in the software. Subsequent analyses were performed using Matlab R2010 (Mathworks, Natick, MA, USA). MEG data were

down-sampled from 1000 to 100 Hz. Heartbeat and EOG artifacts were detected using Independent Component Analysis (ICA) and linearly subtracted from recordings. The ICA decomposition was performed using the Infomax algorithm implemented in the Fieldtrip toolbox (Oostenveld et al., 2011).

Identification of speech edges and extraction of MEG trials

We used a thresholding algorithm to detect temporal edges in each sentence (Gross et al., 2013a). Before applying the algorithm, we rescaled the envelope of each sentence to set its maximum to 1. The envelope of the sentences was obtained from the Hilbert transformed broadband stimulus waveform. The proposed algorithm places edges at the first time-points for which: (1) the average amplitude within a time window of 0.4 s before the time-point is below 0.05; (2) the average amplitude within a time window of 1 s after the time-point is above 0.05; (3) the difference between the average amplitude within a time window from 0.02 s to 0.02 s after the time-point is above 0.05. Following these criteria, we identified a total of 127 onsets (~4 edges per sentence) (*Top-left,* Figure 1). The onsets were confirmed via visual inspection of the rescaled speech envelope.

The preprocessed MEG data time-locked to these edges were segmented into trials of 1.4 s duration beginning 0.4 s before the edge. Trials with MEG peak-to-peak amplitude values lower than 4 pT (magnetometer) or 3 pT/cm (gradiometer) were considered to be free of artifacts. Rejection limits were established prior to data analysis. A minimum of 75% artifact-free trials (95 trials) per participant was required for inclusion in subsequent analyses; all participants were above this threshold. On average, the number of trials retained in the final analysis were 111.6 (range: 96 – 127; SD: 11.1) and 112.6 (range: 96 – 127; SD: 12) for normal and dyslexic, respectively (p = 0.68).

--------- Insert Figure 1 around here ---------

PLV at the sensor level

We used the PLV to evaluate phase synchronization between the artifact-free MEG trials at each sensor *x(t)* and the corresponding speech envelope *y(t)* time-locked to edges. For each participant and time point *t*, the PLV is defined as the absolute value of the circular mean of the phase difference between two signals:

$$\mathbf{PLV}(t) = \left|\langle e^{i(\varphi_x(t)-\varphi_y(t))}\rangle\right|, \quad (1)$$

where $\langle\cdot\rangle$ denotes the mean across trials and $\varphi_x(t)$ and $\varphi_y(t)$ are the instantaneous phase of signal *x(t)* and *y(t)* respectively. The PLV was calculated from 0.4 s before to 1 s after trial onset with a 0.01 s time resolution. The instantaneous phase was estimated with the Hilbert transform. PLV*(t)* quantifies the phase consistency of the oscillatory activity in the MEG response with the speech envelope, time-locked to speech edges. If phases are perfectly aligned across trials the value is 1, and if phases are random the value is 0.

Signals from gradiometer pairs indexed by $r \in \{1, 2, \ldots 102\}$ ($g_{r,1}$ and $g_{r,2}$) were combined to estimate a single, optimal PLV at each time point, as in previous studies (Bourguignon et al., 2015; Lizarazu et al., 2015). Briefly, the signal of virtual gradiometers in the orientation $\theta \in [0; \pi]$ were reconstructed:

$$g_{r,\theta}(t) = g_{r,1}(t)\cos\theta + g_{r,2}(t)\sin\theta, \quad (2)$$

to estimate a PLV that depends on θ:

$$\mathbf{PLV}_{r,\boldsymbol{\theta}}(t) = \left|\langle e^{i(\varphi_{r,\theta}(t)-\varphi_y(t))}\rangle\right|, \quad (3)$$

where $\varphi_{r,\theta}(t)$ is the phase of $g_{r,\theta}(t)$. Final PLV values reported in this article were obtained as

$$\mathbf{PLV}_r(t) = \max_{\theta} \mathbf{PLV}_{r,\boldsymbol{\theta}}(t). \quad (4)$$

Following this procedure, we obtained a PLV for each (i) participant, (ii) MEG gradiometer pair, and (iii) time point.

First, we analyzed the time-dynamics of the PLVs separately for normal and dyslexic readers. For each sensor and time point, the significance of the PLVs was determined with a t-test (1-tailed, equal variance). We used a 1-tailed t-test because we were expecting that speech edges would elicit enhancement of speech-brain phase coupling (Gross et al., 2013a).

The statistical test was performed across subjects, comparing the PLV at each time point after the edge onset with the mean PLV between 0.4 s and 0.2 s before the edge (baseline). The p-values were corrected for multiple comparisons using False Discovery Rate (FDR).

Second, group differences in PLVs were also determined with a t-test (2-tailed, unequal variance). For each sensor and time point, PLVs (baseline corrected) were compared between groups and *p*-values were corrected for multiple comparisons using FDR. Contiguous significant time points were grouped into time windows of interest (W_i). Following this procedure, we obtained a sensor level PLV topographic map for each (i) participant and (ii) W_i.

PLVs at the source level

The forward solution was based on the anatomical MRI (T1) of each individual participant. MRI images were segmented using Freesurfer software (Dale and Sereno, 1993; Fischl, Sereno and Dale 1999). The forward model was based on a single shell boundary element model of the intracranial space obtained with MNE software (Gramfort et al., 2014). It was computed for three orthogonal tangential current dipoles, which were placed on a 1 cm grid covering the whole brain. Then, for each source (three directions), the forward model was reduced to its two principal components of highest singular value, which closely correspond to sources tangential to the skull. The covariance matrix *C* of all N_B sensors was computed from the artifact-free MEG trials. Based on the forward model and *C*, source activity was estimated using a linearly constrained minimum variance beamformer (Van Veen et al., 1997), whose weights at source position r_J are given by

$$w(r_J) = \left[L(r_J)^T C^{-1} L(r_J)\right]^{-1} L(r_J)^T C^{-1}, \quad (5)$$

where $L(r_j)$ is the $N_B \times N_\theta$ leadfield matrix corresponding to sources in the N_θ orthogonal source orientations ($N_\theta \in \{1,2\}$), and a superscript T indicates the matrix transpose.

Source activity during the processing of speech edges was obtained from the matrix product of the spatial filter coefficients arranged in a row vector with the MEG artifact free trials. The PLV between the source activity and speech envelope was obtained for each time point (0.01 s resolution) from 0.4 s before to 1 s after the onset (see formula 1). Then, the average of the PLVs was obtained for each time window of interest (W_i). Finally, the resulting individual PLV maps were normalized to the Montreal Neurological Institute (MNI) brain, by applying a non-linear transformation from individual MRIs to the MNI brain. This transformation was computed using the spatial-normalization algorithm implemented in Statistical Parametric Mapping (SPM8, Wellcome Department of Cognitive Neurology, London, UK). Following this procedure, we obtained a source-level PLV topographic map for each (i) participant and (ii) W_i. Source level PLV maps were compared between groups using a t-test (2-tailed, unequal variance) in each time window. Only significant results ($p < 0.05$ FDR-corrected) were reported.

Correlation analysis between reading, phonological and PLV measures

Correlations between reading skills, phonological skills and PLVs at the source level were conducted separately for the dyslexic and control groups. The PLV measure entered in the correlation analyses was computed as follows. First, we defined a region of interest (ROI) including the sources that showed significant PLV group differences ($p < 0.05$ FDR-corrected) in each time window. Then, the mask defined by the ROI was applied to the PLV source map obtained for each time window of interest (W_i) and participant. Finally, the mean of the masked PLVs was calculated and used as the PLV measure for the correlation analyses.

Results

Behavioral results

Table 1 presents the behavioral results for both normal and dyslexic readers.

--------- Insert Table 1 around here ---------

Intelligence quotient (IQ)

The IQ of all participants was superior to 80 on the WAIS test, suggesting normal intelligence in all our participants. No significant differences were found between groups (p = 0.18).

Reading task

At individual level, we observed that all but three dyslexic participants showed a deficit in pseudoword reading accuracy, whereas none of the control participants did. All dyslexic readers exhibited a deficit in pseudoword reading time ($z < -2$); they were also impaired on word reading time ($z < -1.5$), a measure on which all control participants showed preserved performance.

At the group level, we found a significant group difference in the reading time of words ($p <$ 0.01) and pseudowords (p = 0.03). The average group performance showed that the reading rate of the dyslexic readers for both words and pseudowords was about twice as slow as that of the normal readers (Table 1). In addition to reading more slowly, dyslexic readers also showed significantly lower accuracy rates for reading both words (p = 0.04) and pseudowords (p = 0.02).

Phonological processing tasks

We found a significant group difference (p = 0.02) in accuracy in the pseudoword repetition task, reflecting that dyslexic readers performed the task more poorly than their control peers. Accordingly, the total number of errors was significantly higher in dyslexic readers compared to normal readers (p = 0.01).

On the phonemic deletion task, dyslexic readers were less accurate than normal readers (p = 0.02). The difference in the number of phonemic errors was significantly higher in the dyslexic group than the control group for errors made within (p = 0.01) but not outside the deletion site.

Neurofunctional results

PLVs were significantly higher ($p < 0.01$) during the processing of edges than at baseline in both groups (Figure 1 in Supplementary Material). In normal readers, the PLV enhancement was observed within the [0 – 0.65] s interval in left temporal sensors, and within the [0 – 0.32] s interval in right temporal sensors. In dyslexic readers, the PLV enhancement was observed within the [0 – 0.4] s interval in left temporal sensors, and within the [0 – 0.29] s interval in right temporal sensors.

Importantly, we identified two time windows of interest in which PLVs were significantly higher in skilled readers than in dyslexic readers (*Top* in Figure 2). The first time window (W_1) fell within the [0.15 – 0.44] s interval (all $ps < 0.03$) and the second time window (W_2) within the [0.55 – 0.65] s interval (all $ps < 0.04$). In both time windows, normal readers presented stronger PLVs than dyslexic readers in left temporal sensors (*Bottom* in Figure 2).

--------- Insert Figure 2 around here ---------

The two windows of interest (W_1 = [0.15 – 0.44] s and W_2 = [0.55 – 0.65] s) identified by the sensor-level analyses were further investigated with source reconstruction to highlight the brain regions that showed significant differences between dyslexic and normal readers. In the first time window, , normal readers showed significantly higher ($p < 0.05$ FDR-corrected) PLVs than dyslexic readers in left auditory regions (Brodmann area 42 (BA42) and BA22) (*Left* in Figure 3 and Figure 2 in Supplementary Material). Similar results were observed in the second time window (Figure 3 in Supplementary Material).

--------- Insert Figure 3 around here ---------

ROIs were defined by those sources that showed significant PLV group differences in each time window of interest. For the skilled readers, no significant correlation between the mean of PLVs in these ROIs (see Correlation analysis in Methods) and behavioral tasks was found (all *ps* > 0.23). For dyslexic readers, we observed a negative correlation between the mean PLV of the first (W_1) and second (W_2) time windows and reading times for words (W_1 : r = -0.51, p = 0.04; W_2 : r = -0.49, p = 0.05) and pseudowords (W_1 : r = -0.6, p = 0.01; W_2 : r = -0.53, p = 0.03) (*Right* in Figure 3). Dyslexic readers with the strongest PLVs in the left auditory regions read both words and pseudowords faster. Similarly, we found a positive correlation between the mean of PLVs in the first (W_1) and second (W_2) time windows and reading accuracy for words (W_1 : r = 0.49, p = 0.05; W_2 : r = 0.5, p = 0.05) pseudowords (W_1 : r = 0.48, p = 0.06; W_2 : r = 0.52, p = 0.03). No correlation was found between mean PLV and phonological measures (all *ps* > 0.15).

Discussion

The present study investigates the neural sensitivity of dyslexic readers to speech edges in natural speech. Speech edges represent crucial landmarks that update neural entrainment by realigning the phase of the neural signal with the temporal profile of that specific edge. Previous behavioral data suggest that dyslexia involves a specific deficit in processing the temporal profile of rise times. Here we evaluate dyslexic neural sensitivity to rise times time-locked to speech edges during continuous listening. Evidence for an impairment in synchronizing to speech edges would establish a direct link between the speech tracking deficits observed and the behavioral effects reported for rise time processing.

We observed that all dyslexic readers had difficulties in the pseudoword reading and repetition tasks, where they were slower than controls. These results are in line with previous studies suggesting that a problem with phonological processing is a core marker in dyslexia (Sprenger-Charolles and Serniclaes, 2003; Ramus et al., 2003).

Using phase locking value (PLV) analysis we found that speech edges increased neural synchronization to slow temporal modulations in the speech envelope in bilateral auditory regions across all participants. This synchronization peaks right after the edge (at around 0.1 sec) and slowly decreases across time. Interestingly this peak persists longer in the left auditory regions compared to the homologous right regions, going back to baseline after 0.65 seconds in the left hemisphere and around 0.3 second in the right hemisphere (see a similar pattern of data in Gross et al., 2013a). Interestingly, this sustained left-lateralized effect has been interpreted as evidence "*that speech continuously entrains brain rhythms beyond a stereotypical short-lived phase reset evoked by edges*" (page 11, Gross et al., 2013a). In other words, this effect has been interpreted as evidence for prolonged entrainment following phase reset to speech edges. This more sustained effect in the left hemisphere could potentially reflect increased attentional resources deployed for tracking the speech envelope. Vander Ghinst et al. (2016) reported

increased left hemisphere involvement for delta band cortical speech tracking in noisy compared to noiseless conditions (where the effect was mostly right lateralized). This left lateralization could mirror increased attentional demands imposed by tracking speech in noise. It could also be related to the integration of phonemic information, i.e. combined response and interaction of different phonemes and features in the speech signal. In fact, interhemispheric differences in sensitivity to temporal and spectral sound properties (Zatorre and Belin, 2001; Poeppel, 2003; Boemio et al., 2005) have been suggested to predispose left auditory regions for the representation of phonemic information based on acoustic phonetic information.

Importantly, dyslexic participants do not show this later effect. Figure 2 (see also Supplementary Figure 1) shows that synchronization to edges is short lived in both left and right auditory cortices in dyslexic readers. Their initial response is not reliably different from control participants, showing that dyslexic participants reset their neural oscillations to speech edges as efficiently as the control group. However, this initial reset is not followed by the prolonged oscillatory tracking of following syllables, as observed in controls. Group differences emerged in two time windows (i.e. from 0.15 to 0.44 s and from 0.55 to 0.65 s), but they probably comprise one large window. Actually, the group effect between 0.45 s and 0.54 s was significant before applying FRD correction, thus we would probably have observed a single window if we had used a less conservative statistical method.

The lack of any group difference right at the onset of the speech edge might seem at odds with behavioral evidence that dyslexics present a specific deficit in processing rise-time envelope information. However, the temporal course of the differential group effect that we observed speaks for an oscillatory tracking of individual syllables that efficiently resets at the edges, but rapidly decays over the following syllables. It is possible that, in natural speech listening, rise-time differential processing is only evident if syllables are not at the edges and, consequently are less perceptually salient. Such reduced perceptual saliency renders oscillatory tracking more difficult and this increased difficulty specifically impacts dyslexic populations, affecting syllabic

entrainment that *follows* speech edges. One potential way to test this explanation is to study speech-in-noise tracking in dyslexia and evaluate if, under such circumstances, the differential PLV effect already emerges at the edge (Van Hirtum et al., 2019a, b).

This group difference is left lateralized and localized in the left temporal regions, close to the auditory cortex. The left-lateralization of this PLV effect seems at odds with previous studies that showed atypical right hemisphere responses to slow temporal modulations in dyslexic readers (Cutini et al., 2015; Molinaro et al., 2016). Using functional near-infrared spectroscopy (fNIRS), Cutini et al. (2015) found that dyslexic readers showed atypical HbO (oxygenated hemoglobin) concentration indices during the processing of 2 Hz AM white noise in the right supramarginal gyrus region. This study used non-linguistic stimuli and measured changes in oxygenated blood flow, which is not a direct measurement of the neural entrainment. Thus, results from Cutini et al. (2015) are hardly comparable with our findings. Furthermore, the study of Cutini and colleagues (2015) involved children and not adults. Lateralization towards the left hemisphere could change with age or with reading experience, or even with language experience. Given that the task used in the present study was a speech listening comprehension task, it is not clear that access to phonemic representations is actually required for participants to perform the task. However, we already know that phonemic representations get stronger and reading gets more left-lateralized in terms of the neural activity strength as participants gain more reading experience (Turkeltaub et al., 2003). As the participants in the current study are adults, we cannot tell the developmental antecedents of the laterality difference that is observed. Interestingly, Molinaro et al. (2016) reported reduced delta band coherence in dyslexic readers compared to controls for the same group of participants. The effects were located in the right auditory cortex and left hemisphere but were found in more frontal regions than those reported here. While the coherence analysis performed previously reflects a more global measure of speech-brain coupling, here we focus on those specific parts of the speech input (i.e., edges) assumed to be crucial landmarks for maintaining a high level of temporal precision between

brain oscillations and the temporal structure of speech. In dyslexic readers, synchronization levels in left temporal regions were negatively correlated with reading times for pseudowords, for which higher synchronization is associated with lower reading times. Pseudoword reading requires mapping between graphemes and phonemes, an ability that is prototypically impaired in dyslexia. Interestingly, we did not find correlations between synchronization values and scores from the non-word repetition task. The non-word repetition task heavily taxes auditory attention (Coady and Evans, 2008). Thus, we suggest that auditory attention is not a good explanation for the current findings. The timing (~ 0.15 to 0.55 s after trial onset) and the leftward lateralization of group effects, could be associated with difficulties in processing phonemic information in dyslexia. Atypical synchronization to slow rhythms triggered by speech edges in our dyslexic participants may underlie their difficulties in integrating the phonemic speech content that followed these edges. Indeed, numerous studies have shown that dyslexic readers make more errors than normal readers when they are asked to discriminate pairs of edges which only differ in one phonemic feature, such as /pa/ and /ba/ (Reed, 1989; Masterson, Hazan and Wijayatilake, 1995; Mody, Studdert-Kennedy, Brady, 1997; Adlard and Hazan, 1998). Reduced sensitivity to slow rhythms might impair the processing of fast phonemic-rate information in dyslexia, which is supported by a left-sided oscillatory network (Poelmans et al., 2012; Lehongre et al., 2013). In fact, atypical neural entrainment in the delta and theta bands could disrupt hierarchical coupling between the low-frequency (delta-theta) phase and the amplitude of high-frequency (gamma) oscillations observed in the auditory regions of the left hemisphere (Gross et al., 2013a). In line with this proposal, Lizarazu et al. (2015) showed atypical oscillatory responses to amplitude-modulated stimuli at both low- (4 Hz) and high- (30 Hz) frequency bands within the same dyslexic participants. These deficits were respectively associated with atypical right and left hemispheric specialization.

No significant correlations were found between the PLV to edges and behavioral tasks in control readers. We found two possible explanations for this lack of relationship. The low variability of

behavioral scores could explain the low correlation values found for the control group. As we observed in Table 1, the SD and the range of behavioral scores for reading and phonological tasks was lower for the control than the dyslexic group. For example, for word reading times, the SD and range of the scores in the control group were 8.1 and 19 – 45 s respectively, whereas in the dyslexic group these values were 50.1 and 23 – 190 s. This is probably because in the present study, control readers were adults and their reading skills were fully established. Another possible explanation is that once neural synchronization to edges peaked to a point within the "typical" range, their relationship to behavioral scores was no longer apparent. Dyslexic readers that were closer to this ceiling PLV were the ones that showed better reading scores (they were faster and made less errors). One way to shed light on this question would be to include less proficient control readers (i.e. children with different reading levels). In this way, we could increase the variability of the behavioral scores and analyze the evolution of the PLV to edge relationship with increasing reading proficiency.

One limitation of the present study is the lack of a behavioural task to measure rise-time discrimination in dyslexic readers. This task would have allowed us to determine if there is a mechanistic connection between the atypical neural response and reduced sensitivity to edges in dyslexia (Goswami et al., 2002, 2011; Richardson et al., 2004; Thomson and Goswami, 2008; Thomson, Goswami and Baldeweg, 2009). If no group differences in rise-time were found, that would be even more interesting. This latter result would suggest that in adult populations atypical neural processing present from birth (Goswami, 2011) can be masked at the behavioural level while atypical brain responses persist (van Hirtum et al., 2019a, b). Another limitation of the present study is that, although we checked that all participants had normal hearing (passed the hearing tests), we did not measure the specific sensitivity of each them. Individual differences in the hearing sensitivity is a source of variance that is present in our data. Future research is needed to better characterize the atypical synchronization to speech edges in dyslexia. For example, by designing an experiment that controlled and manipulated for the

different types of edges according to their position (e.g., at voiceless plosives, or at the start of vowel sounds).

Altogether, these results highlight the importance of low-frequency neural oscillations for processing edges in the left hemisphere. As mentioned above, during speech processing, low-frequency (delta and theta band) oscillations modulate higher-frequency (gamma band) oscillations, at the scale of phonemic information (Gross et al., 2013a; Lizarazu, Lallier and Molinaro, 2019). Short-lived synchronization of low-frequency oscillations to speech edges in the left hemisphere could reduce sensitivity to phonemic information in dyslexia (Poelmans et al., 2012; Lehongre et al., 2011, 2013). There thus appears to be a link between the phonological disorder observed in dyslexia and prolonged tracking time-locked to speech edges in left temporal regions.

Conclusion

Results from this study showed that, in normal readers, speech edges enhanced the entrainment of low-frequency (delta and theta) oscillations from 0 to 0.65 s and from 0 to 0.32 s after the edge onset in the left and right temporal regions, respectively. We suggest that the neural mechanism underlying processing of speech edges is affected in dyslexia. Dyslexic readers showed weaker synchronization of low-frequency oscillations to speech edges than control readers in left auditory regions. Atypical response of low-frequency oscillations to speech edges could impair higher frequency oscillations in a left -side oscillatory network, leading to difficulties with phonological processing and reading in dyslexia.

Acknowledgments

This work was supported by: the Basque Government through the BERC 2018-2021 program and by the Spanish State Research Agency through BCBL Severo Ochoa excellence accreditation SEV-2015-0490. The Spanish Ministry of Science and Innovation (CONSOLIDER-INGENIO2010 and CSD2008-00048 to M.C.), the European Research Council (ERC-2011-ADG-295362 to M.C.), the Spanish Ministry of Economy and Competitiveness (MINECO), Programme d'investissements d'avenir (ANR-10-LABX-0087 and ANR-10-IDEX-0001-02 to M.L), the Agencia Estatal de Investigación (AEI), the Fondo Europeo de Desarrollo Regional (FEDER) (PSI2012-32128 to M.L., PSI2016-77175-P to M.B., PSI2015-67353-R to M.C., RTI2018-096311-B-I00 to N.M.), and Innoviris (grant Attract 2015-BB2B-10 to M.B.). The BCBL acknowledges funding from Ayuda Centro de Excelencia Severo Ochoa SEV-2015-0490 from the MINECO. The authors would like to specifically thank all the families who took part in this study.

Research transparency

No part of the study procedures or analyses was preregistered prior to the research being undertaken. We reported how we determined our sample size, all inclusion/exclusion criteria, all data exclusions, whether inclusion/exclusion criteria were established prior to data analysis, all manipulations, and all measures in the study. Matlab based scripts for data analysis, experiment code and stimuli are archived at the following link: https://osf.io/5p32q/ (DOI 10.17605/OSF.IO/5P32Q). Legal copyright restrictions prevent public archiving of the WAIS and PROLEC-R battery, which can be obtained from the cited references. The conditions of our ethics approval do not permit public archiving of the data obtained in this study. Readers seeking access to the data should contact the lead author Mikel Lizarazu (m.lizarazu@bcbl.eu) or the local ethics committee at the Basque Center on Cognition Brain and Language (BCBL). Access will be granted to named individuals in accordance with ethical procedures governing

the reuse of sensitive data. Specifically, requestors will complete a data sharing agreement before accessing data.

References

Adlard A, Hazan V. 1998. Speech perception in children with specific reading difficulties (dyslexia). Quarterly Journal of Experimental Psychology 51, 153–177.

Boemio A, Fromm S, Braun A, Poeppel D. 2005. Hierarchical and asymmetric temporal sensitivity in human auditory cortices. Nature Neuroscience 8(3), 389-395.

Boersma P, Weenink D. 2018. Praat: Doing phonetics by computer [Computer program]. Version 6.0. 37. RetrievedFebruary 3, 2018.

Bourguignon M, De Tiege X, de Beeck MO, Ligot N, Paquier P, Van Bogaert P, Goldman S, Hari R, Jousmäki V. 2013. The pace of prosodic phrasing couples the listener's cortex to the reader's voice. Human Brain Mapping 34(2), 314-326.

Bourguignon M, Piitulainen H, De Tiège X, Jousmäki V, Hari R. 2015. Corticokinematic coherence mainly reflects movement-induced proprioceptive feedback. Neuroimage 106, 382-390.

Castles A, Coltheart M. 1993. Varieties of developmental dyslexia. Cognition 47(2), 149-180.

Coady JA, Evans JL. 2008. Uses and interpretations of non‐word repetition tasks in children with and without specific language impairments (SLI). International Journal of Language & Communication Disorders 43(1), 1-40.

Cuetos F, Rodríguez B, Ruano E, Arribas D. 2007. Batería de evaluación de los procesos lectores. Revisada (PROLEC-R). Madrid: TEA.

Cutini S, Szűcs D, Mead N, Huss M, Goswami U. 2016. Atypical right hemisphere response to slow temporal modulations in children with developmental dyslexia. Neuroimage, 143, 40-49.

Dale AM, Sereno MI. 1993. Improved localization of cortical activity by combining EEG and MEG with MRI cortical surface reconstruction: a linear approach. Journal of Cognitive Neuroscience 5(2), 162-176.

De Vos A, Vanvooren S, Vanderauwera J, Ghesquière P, Wouters J. 2017a. Atypical neural synchronization to speech envelope modulations in dyslexia. Brain and Language 164, 106-117.

De Vos A, Vanvooren S, Vanderauwera J, Ghesquière P, Wouters J. 2017b. A longitudinal study investigating neural processing of speech envelope modulation rates in children with (a family risk for) dyslexia. Cortex 93, 206-219.

Doelling KB, Arnal LH, Ghitza O, Poeppel D. 2014. Acoustic landmarks drive delta–theta oscillations to enable speech comprehension by facilitating perceptual parsing. Neuroimage 85, 761-768.

Donhauser PW, Baillet S. 2019. Two Distinct Neural Timescales for Predictive Speech Processing. Neuron.

Fischl B, Sereno MI, Dale AM. 1999. Cortical surface-based analysis: II: inflation, flattening, and a surface-based coordinate system. Neuroimage 9(2), 195-207.

Goswami U. 2011. A temporal sampling framework for developmental dyslexia. Trends in Cognitive Sciences 15(1), 3-10.

Goswami U, Thomson J, Richardson U, Stainthorp R, Hughes D, Rosen S, Scott SK. 2002. Amplitude envelope onsets and developmental dyslexia: A new hypothesis. Proceedings of the National Academy of Sciences 99(16), 10911-10916.

Gramfort A, Luessi M, Larson E, Engemann DA, Strohmeier D, Brodbeck C, Parkkonen L, Hämäläinen MS. 2014. MNE software for processing MEG and EEG data. Neuroimage 86, 446-460.

Greenberg S, Carvey H, Hitchcock L, Chang S. 2003. Temporal properties of spontaneous speech—a syllable-centric perspective. Journal of Phonetics 31(3-4), 465-485.

Gross J, Hoogenboom N, Thut G, Schyns P, Panzeri S, Belin P, Garrod S. 2013a. Speech rhythms and multiplexed oscillatory sensory coding in the human brain. PLoS Biology 11(12), e1001752.

Gross J, Baillet S, Barnes GR, Henson RN, Hillebrand A, Jensen O, Jerbi K, Litvak V, Maess B, Oostenveld R, Parkkonen L, Taylor JR, van Wassenhove V, Wibral M, Schoffelen JM. 2013b. Good practice for conducting and reporting MEG research. Neuroimage, 65, 349-363.

Hämäläinen M, Hari R, Ilmoniemi RJ, Knuutila J, Lounasmaa OV. 1993. Magnetoencephalography—theory, instrumentation, and applications to noninvasive studies of the working human brain. Reviews of Modern Physics, 65(2), 413.

Hämäläinen JA, Rupp A, Soltész F, Szücs D, Goswami U. 2012. Reduced phase locking to slow amplitude modulation in adults with dyslexia: an MEG study. Neuroimage 59(3), 2952-2961.

Jiménez-Bravo M, Marrero V, Benítez-Burraco A. 2017. An oscillopathic approach to developmental dyslexia: from genes to speech processing. Behavioural Brain Research 329, 84-95.

Lehongre K, Ramus F, Villiermet N, Schwartz D, Giraud AL. 2011. Altered low-gamma sampling in auditory cortex accounts for the three main facets of dyslexia. Neuron 72(6), 1080-1090.

Lehongre K, Morillon B, Giraud AL, Ramus F. 2013. Impaired auditory sampling in dyslexia: further evidence from combined fMRI and EEG. Frontiers in Human Neuroscience 7, 454.

Leong V, Goswami U. 2014. Impaired extraction of speech rhythm from temporal modulation patterns in speech in developmental dyslexia. Frontiers in Human Neuroscience 8, 96.

Leong V, Goswami U. 2015. Acoustic-emergent phonology in the amplitude envelope of child-directed speech. PloS one 10(12), e0144411.

Lizarazu M, Lallier M, Molinaro N, Bourguignon M, Paz‐Alonso PM, Lerma‐Usabiaga G, Carreiras M. 2015. Developmental evaluation of atypical auditory sampling in dyslexia: Functional and structural evidence. Human Brain Mapping 36(12), 4986-5002.

Lizarazu M, Lallier M, Molinaro N. 2019. Phase−amplitude coupling between theta and gamma oscillations adapts to speech rate. Annals of the New York Academy of Sciences 1453(1), 140.

Manis FR, Seidenberg MS, Doi LM, McBride-Chang C, Petersen A. 1996. On the bases of two subtypes of development dyslexia. Cognition 58(2), 157-195.

Masterson J, Hazan V, Wijayatilake L. 1995. Phonemic processing problems in developmental dyslexia. Cognitive Neuropsychology 12, 233-259.

Meyer L, Sun Y, Martin AE. 2019. Synchronous, but not entrained: exogenous and endogenous cortical rhythms of speech and language processing. Language, Cognition and Neuroscience 1-11.

Mody M, Studdert-Kennedy M, Brady S. 1997. Speech perception deficits in poor readers: Auditory processing or phonological coding? Journal of Experimental Child Psychology 64, 199-231.

Molinaro N, Lizarazu M, Lallier M, Bourguignon M, Carreiras M. 2016. Out-of-synchrony speech entrainment in developmental dyslexia. Human Brain Mapping 37(8), 2767-2783.

Molinaro N, Lizarazu M. 2018. Delta (but not theta)-band cortical entrainment involves speech-specific processing. European Journal of Neuroscience 48(7), 2642-2650.

Obleser J, Kayser C. 2019. Neural entrainment and attentional selection in the listening brain. Trends in Cognitive Sciences.

Oostenveld R, Fries P, Maris E, Schoffelen JM. 2011. FieldTrip: open source software for advanced analysis of MEG, EEG, and invasive electrophysiological data. Computational Intelligence and Neuroscience 1.

Poelmans H, Luts H, Vandermosten M, Boets B, Ghesquière P, Wouters J. 2012. Auditory steady state cortical responses indicate deviant phonemic-rate processing in adults with dyslexia. Ear and Hearing 33(1), 134-143.

Poeppel D. 2003. The analysis of speech in different temporal integration windows: cerebral lateralization as ‘asymmetric sampling in time’. Speech Communication 41(1), 245-255.

Poeppel D, Idsardi WJ, Van Wassenhove V. 2008. Speech perception at the interface of neurobiology and linguistics. Philosophical Transactions of the Royal Society B: Biological Sciences 363(1493), 1071-1086.

Power AJ, Mead N, Barnes L, Goswami U. 2013. Neural entrainment to rhythmic speech in children with developmental dyslexia. Frontiers in Human Neuroscience 7, 777.

Power AJ, Colling LC, Mead N, Barnes L, Goswami U. 2016. Neural encoding of the speech envelope by children with developmental dyslexia. Brain and Language 160, 1–10.

Ramus F, Rosen S, Dakin SC, Day BL, Castellote JM, White S, Frith U. 2003. Theories of developmental dyslexia: insights from a multiple case study of dyslexic adults. Brain 126(4), 841-865.

Reed MA. 1989. Speech perception and the discrimination of brief auditory cues in dyslexic children. Journal of Experimental Child Psychology 48, 270-292.

Richardson U, Thomson JM, Scott SK, Goswami U. 2004. Auditory processing skills and phonological representation in dyslexic children. Dyslexia 10(3), 215-233.

Sohrabi A, Sohrabi S. 2017. Normal and abnormal reading: Phonology and Dyslexia. Reading Research Journal 1(1), 99- 112.

Sprenger-Charolles L, Serniclaes W. 2003. Reliability of phonological and surface subtypes in developmental dyslexia: A review of five multiple cases studies. Current Psychology Letters. Behaviour, Brain & Cognition, (10, Vol. 1, 2003).

Sprenger-Charolles L. 2011. Dyslexia subtypes in languages differing in orthographic transparency: English, French and Spanish. Escritos de Psicología 4(2), 5-16.

Taulu S, Kajola M. 2005. Presentation of electromagnetic multichannel data: the signal space separation method. Journal of Applied Physics 97(12), 124905.

Thomson JM, Goswami U. 2008. Rhythmic processing in children with developmental dyslexia: auditory and motor rhythms link to reading and spelling. Journal of Physiology-Paris 102(1-3), 120-129.

Thomson JM, Goswami U, Baldeweg T. 2009. The ERP signature of sound rise time changes. Brain Research 1254, 74-83.

Turkeltaub PE, Gareau L, Flowers DL, Zeffiro TA, Eden GF. 2003. Development of neural mechanisms for reading. Nature neuroscience 6(7), 767-773.

Vander Ghinst M, Bourguignon M, de Beeck MO, Wens V, Marty B, Hassid S, Choufani G, Jousmäki V, Hari R, Van Bogaert P and others. 2016. Left superior temporal gyrus is coupled to attended speech in a cocktail-party auditory scene. Journal of Neuroscience 36(5), 1596-1606.

Van Hirtum T, Moncada-Torres A, Ghesquière P, Wouters, J. 2019a. Speech envelope enhancement instantaneously effaces atypical speech perception in dyslexia. Ear and Hearing 40(5), 1242-1252.

Van Hirtum T, Ghesquière P, Wouters J. 2019b. Atypical neural processing of rise time by adults with dyslexia. Cortex 113, 128-140.Van Veen BD, Van Drongelen W, Yuchtman M, Suzuki A. 1997. Localization of brain electrical activity via linearly constrained minimum variance spatial filtering. IEEE Transactions on Biomedical Engineering 44(9), 867-880.

Wechsler D. 2008. Wechsler adult intelligence scale-fourth. San Antonio, TX: The Psychological Corporation Google Scholar.

Zatorre RJ, Belin P. 2001. Spectral and temporal processing in human auditory cortex. Cerebral Cortex 11(10), 946-953.

Tables

Table 1.

IQ, reading and phonological skills in the two participant groups. Measures showing significant group differences are marked with an asterisk (*).

	Normal Readers (N = 16)		Dyslexic Readers (N = 16)	
	M(SD)	Range	M(SD)	Range
IQ (standard Score)	121 (9)	104 - 131	117(7)	101 - 127
Reading tasks				
Word reading				
Accuracy (/40) (*)	39.6 (0.6)	38 - 40	37.3 (3.2)	29 - 40
Time [s] (*)	25.8 (8.1)	19 - 45	68.6 (50.1)	23 - 190
Pseudoword reading				
Accuracy (/40) (*)	39.0 (1.4)	36 - 40	32.8 (5.2)	19 - 40
Time [s] (*)	42.5 (10.4)	32 - 68	81.3 (31.2)	43 - 120
Phonological processing tasks				
Pseudoword repetition				
Total Accuracy [%] (*)	91.5 (7.1)	74.8 - 100	81.6 (8.4)	68 - 91
No. of phonemic permutation errors	0.1 (0.5)	0 - 3	0.5 (0.7)	0 - 2
No. of phonemic addition errors	0.2 (0.3)	0 - 1	6.4 (3.6)	0 - 3
No. of phonemic substitution errors	1.9 (2)	0 - 8	4.3 (2.9)	1 - 13
No. of phonemic omission errors	0.6 (0.7)	0 - 3	0.8 (1.2)	0 - 5
Phonemic deletion				
Total Accuracy [%] (*)	92.5 (11.2)	64.5 - 100	77.5 (21)	0 - 100
No. of deletion errors (*)	1.5 (2.3)	0 - 8	3.4 (4.1)	0 - 13
No. of error out of deletion site	0.5 (1)	0 - 3	2.3 (2.7)	0 - 10

Figure Captions

Figure 1:

Pipeline of the PLV analyses. *Top-left*: The speech signal of a sentence presented auditorily to the participants in the MEG. The envelope of the speech signals was extracted using the Hilbert transform. The edge onsets in the speech envelope were identified using an algorithm developed by Gross et al., 2003a. *Top-right*: Location of the MEG sensors. MEG signals were preprocessed using the signal space separation (SSS) method to correct for head movements and magnetic interferences during the recording. The preprocessed MEG data time-locked to onsets were segmented into trials of 1.4 s duration beginning 0.4 s before the onset. *Bottom*: Then, the Phase locking value (PLV) was computed to evaluate coupling between the speech segments and the MEG trials during edge processing. Phase synchronization was calculated at the sensor level and the effects were projected to the source space using a linear constrained minimum variance (LCMV) beamformer. Abbreviations: L, left hemisphere; R, right hemisphere.

Figure 2:

Sensor level analysis of the PLVs. *Top:* The graphs on the left and right show the evolution of the PLVs (baseline corrected, mean of the PLVs in the [-0.4 – -0.2] s interval) in the window of interest in a representative channel from the left (L) (MEG0212/3) and right (R) (MEG1332/3) hemispheres, respectively. Blue and red shadows represent the standard error area of the PLVs in controls (C) and dyslexics (D), respectively. Grey boxes represent time points where the PLVs are significantly higher (*, $p < 0.05$ FDR-corrected) in C than in D. Two windows of interest were identified in the L hemisphere: window 1 (W_1 = [0.15 – 0.44] s) and window 2 (W_2 = [0.55 – 0.65] s). *Bottom:* Sensor maps of the mean PLVs (baseline corrected) during the processing of speech edges in W_1 and W_2 in C and D. Sensor maps of the PLV differences between groups in W_1 and W_2 are also plotted. Sensors showing significant differences ($p < 0.05$, FDR-corrected) are highlighted.

Figure 3:

Source level analysis of the PLVs in the first time window (W_1). *Left*: Statistical map (p-values) representing sources that showed significant ($p < 0.05$, FDR-corrected) PLV group differences in W_1. The highlighted sources constituted the ROI. *Right*: The correlation between pseudoword reading times (RT) and PLVs in the ROI for dyslexic readers in the W_1.

Figure 1:

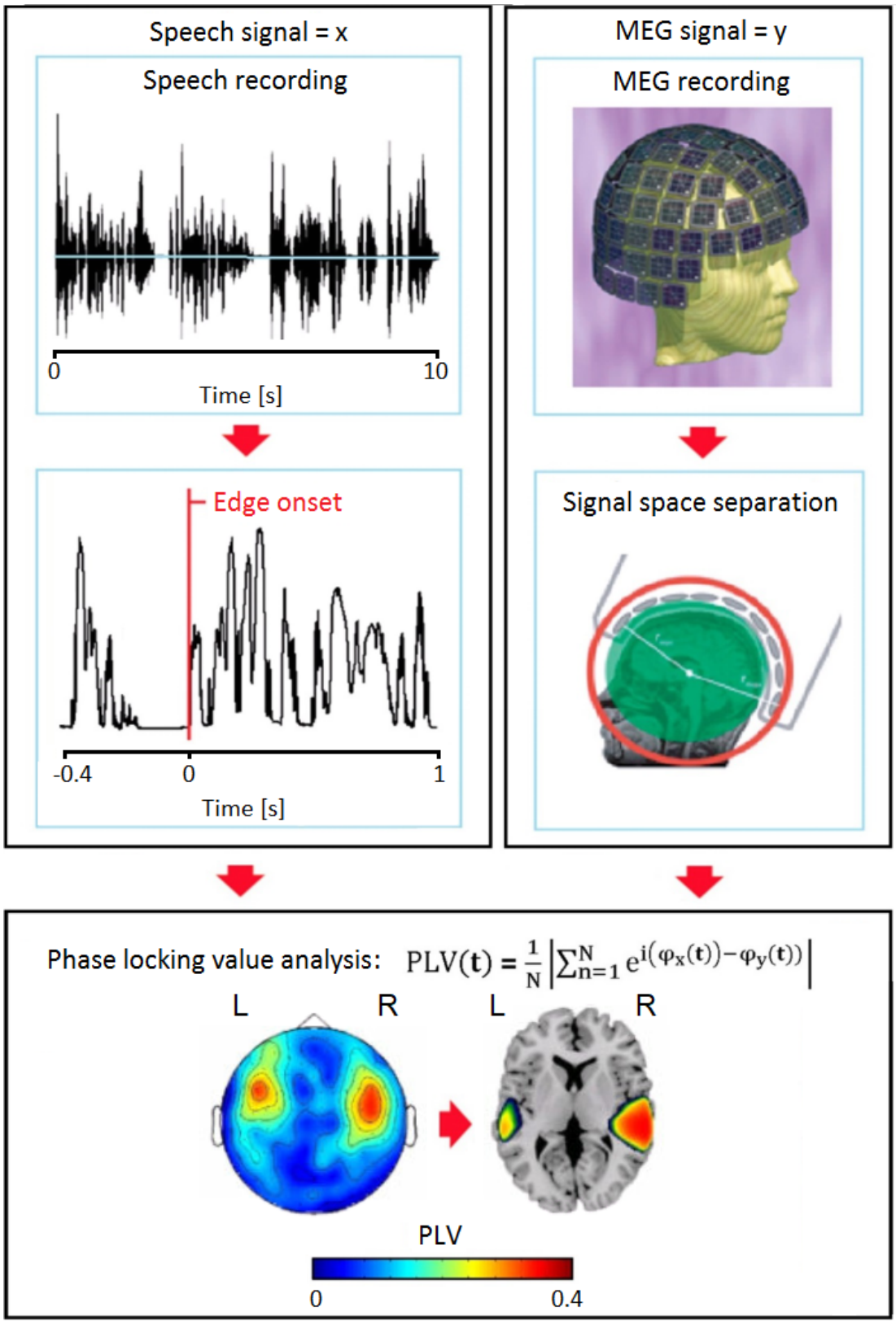
Speech signal = x
Speech recording
0
10
Time [s]
Edge onset
-0.4
0
1
Time [s]
MEG signal = y
MEG recording
Signal space separation
Phase locking value analysis: $PLV(t) = \frac{1}{N}\left|\sum_{n=1}^{N} e^{i(\varphi_x(t))-\varphi_y(t))}\right|$
L
R
L
R
PLV
0
0.4

Figure 2:

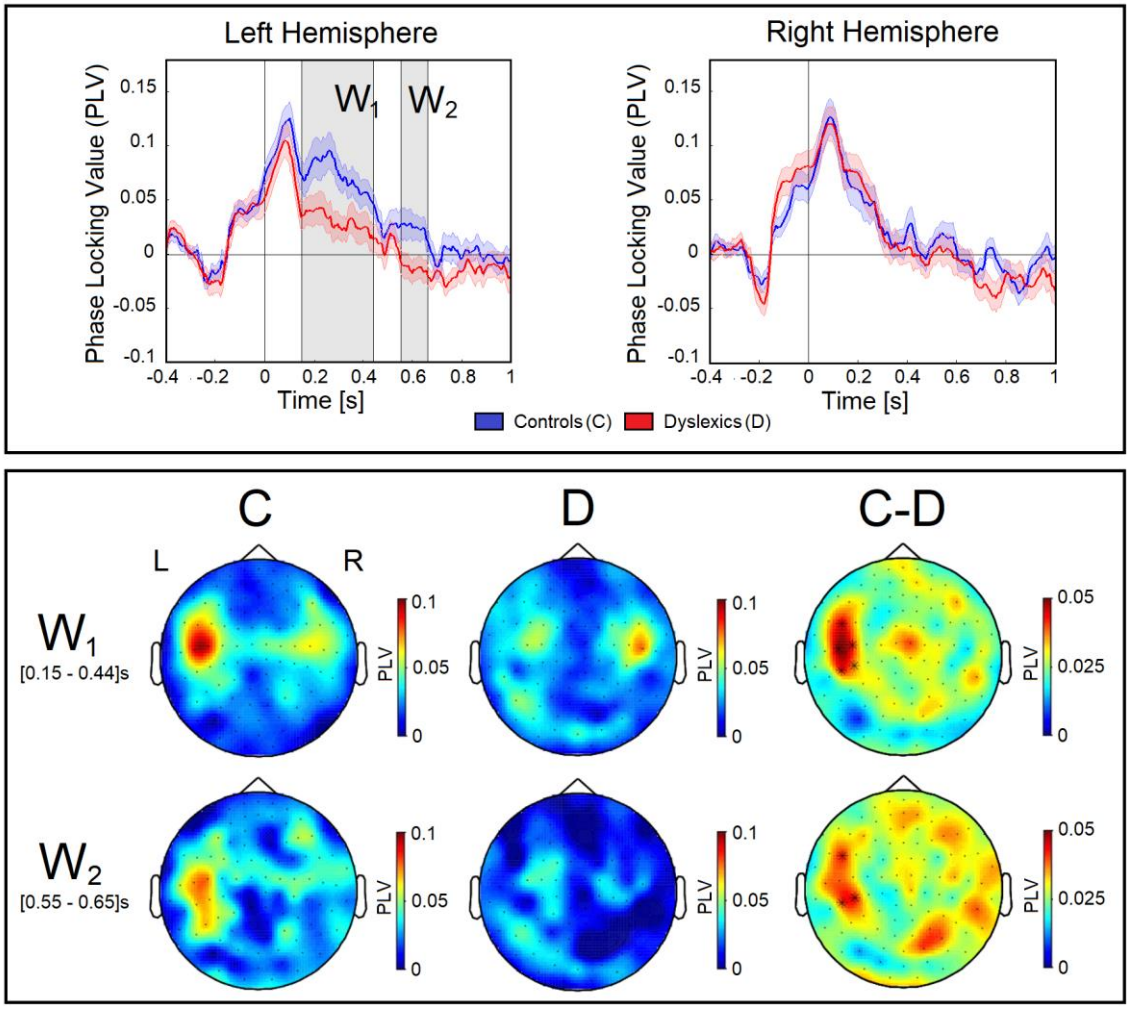

Figure 3:

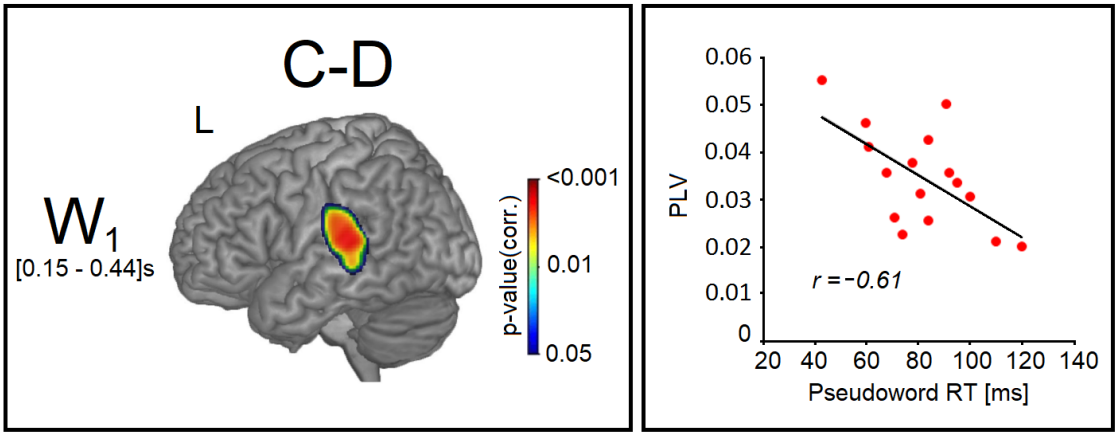

Supplementary Figure 1:

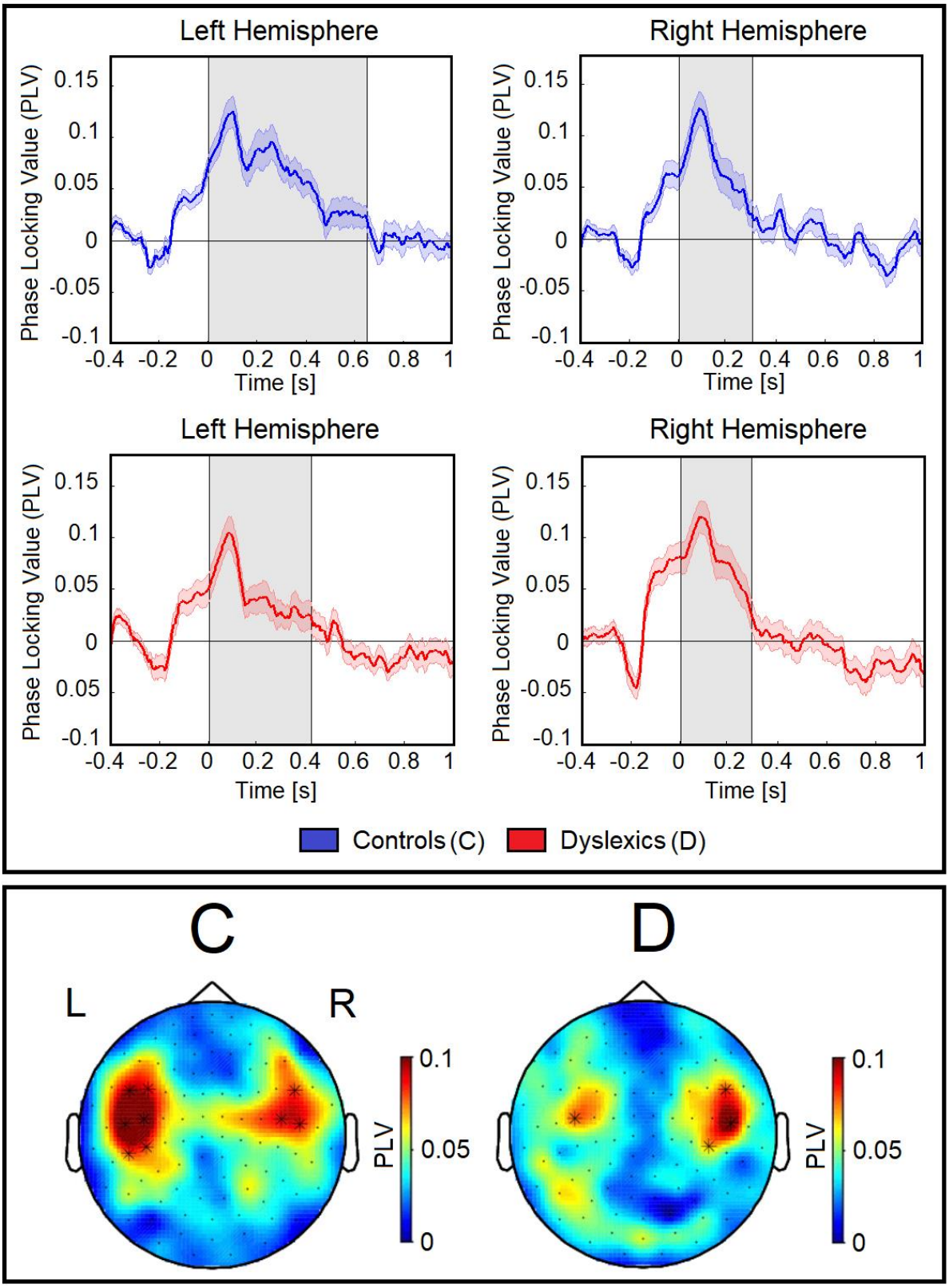

Supplementary Figure 2:

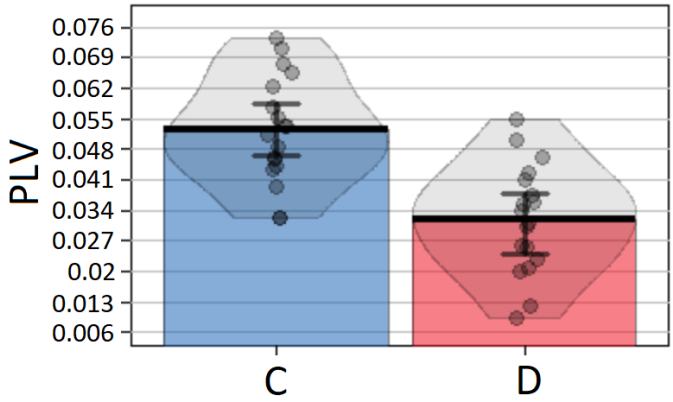

Supplementary Figure 3: